Published in final edited form as:

*Nat Commun*. 2012 ; 3: 1172. doi:10.1038/ncomms2144.

# Opposing regulation of dopaminergic activity and exploratory motor behavior by forebrain and brainstem cholinergic circuits

**Jyoti C. Patel**[1], **Elsa Rossignol**[2,#], **Margaret E. Rice**[1,*], and **Robert P. Machold**[2,3,*]

[1]Department of Neurosurgery and Department of Physiology and Neuroscience, NYU School of Medicine, New York, NY 10016

[2]Smilow Neuroscience Program, NYU School of Medicine, New York, NY 10016

[3]Department of Otolaryngology, NYU School of Medicine, New York, NY 10016

## Abstract

Dopamine transmission is critical for exploratory motor behavior. A key regulator is acetylcholine: forebrain acetylcholine regulates striatal dopamine release, whereas brainstem cholinergic inputs regulate the transition from tonic to burst firing modes of dopamine neurons. How these sources of cholinergic activity combine to control dopamine efflux and exploratory motor behavior is unclear. Here we show that mice lacking total forebrain acetylcholine exhibit enhanced frequency dependent striatal dopamine release and are hyperactive in a novel environment, whereas mice lacking rostral brainstem acetylcholine are hypoactive. Exploratory motor behavior is normalized by removal of both cholinergic sources. Involvement of dopamine in the exploratory motor phenotypes observed in these mutants is indicated by their altered sensitivity to the dopamine D2 receptor antagonist raclopride. These results support a model in which forebrain and brainstem cholinergic systems act in tandem to regulate striatal dopamine signaling for proper control of motor activity.

Dopamine (DA) transmission has been implicated in a variety of motor, emotional, and cognitive functions[1–3]. Midbrain DA neurons in the substantia nigra pars compacta (SNc) and ventral tegmental area (VTA) provide important modulatory input to the striatal complex, including the caudate putamen (CPu) and nucleus accumbens (NAc). Acetylcholine (ACh) signaling pathways regulate DA efflux within the striatum at two fundamental levels of the circuit[4]. First, the burst firing of DA neurons in the SNc and VTA is stimulated perisomatically by glutamatergic and cholinergic inputs from the pedunculopontine tegmental (PTg) and laterodorsal tegmental (LDTg) nuclei in the rostral brainstem[5–7], thereby resulting in increased striatal DA efflux[6] and locomotor activity[8]. In

*Correspondence and requests for materials should be addressed to R.P.M (robert.machold@nyumc.org) or M.E.R. (margaret.rice@nyu.edu).

#present address: Pediatric Neurology, Centre Hospitalier Universitaire (CHU) Ste-Justine, Montreal, Quebec, Canada

**Author Contributions**

R.P.M. designed, generated and genotyped the mice and performed the histological analyses. J.C.P. and M.E.R. designed, performed and analyzed the DA release experiments. R.P.M. and E.R. designed, performed and analyzed the behavioral experiments. All authors interpreted the data and wrote the manuscript.

**Conflict of interest**

The authors declare no competing financial interests.

particular, cholinergic inputs from the LDTg appear to act as a gate for the transition from tonic to burst firing modes, thereby regulating the responsiveness of DA neurons to glutamatergic signaling[9]. Second, ACh release from striatal cholinergic interneurons can trigger DA release via presynaptic nicotinic ACh receptors (nAChRs) on DA axons[10–12]. Inhibition or desensitization of nAChRs on DAergic axons in striatal slices leads to a decrease in DA release evoked by a single stimulus pulse, but an increase in release evoked at burst-like frequencies, thus amplifying the frequency dependence of axonal DA release as monitored by fast-scan cyclic voltammetry (FCV)[13,14]. While striatal ACh can also affect the excitability of medium spiny neurons directly by signaling through muscarinic ACh receptors (mAChRs)[15], intrastriatal injections of scopolamine, a mAChR antagonist, does not alter motor activity[16]. In addition to local cholinergic regulation of DA efflux within the striatum, ACh arising from projection neurons within the ventral forebrain (e.g., nucleus basalis of Meynert) likely regulates striatal DA efflux indirectly via modulation of descending glutamatergic pathways from the prefrontal cortex, ventral pallidum, and hippocampus to the SNc/VTA[17,18]. Thus, we hypothesized that broad removal of ACh within the forebrain would result in exaggerated striatal DA signaling and altered motor behaviors in a manner dependent on the stimulation of burst firing of midbrain DA neurons by brainstem-derived ACh.

To test the relative contributions of forebrain and brainstem cholinergic input to the regulation of DAergic activity, we took advantage of genetic ablation strategies in mice to eliminate ACh synthesis selectively in the forebrain, brainstem, or both regions simultaneously. We then assessed the effects on evoked striatal DA release *in vitro*, and the behavioral propensity for open field exploration when placed in a novel environment, which is highly responsive to changes in striatal DA efflux[19,20]. We found that mice lacking forebrain ACh showed enhanced phasic-to-tonic DA release throughout the striatal complex, and exhibited locomotor hyperactivity in a novel environment. By contrast, exploratory motor behavior was reduced in mice lacking brainstem ACh, consistent with a predicted decrease in DA neuron burst firing, with lower striatal DA signaling indicated by a lack of sensitivity to the DA D2 receptor antagonist raclopride. Remarkably, exploratory motor behavior was normalized in mice lacking both forebrain and brainstem ACh. These findings highlight the critical roles that forebrain and brainstem cholinergic systems play in driving striatal DAergic activity for the control of exploratory motor activity.

## Results

### Generation of forebrain ACh knock-out mice

The enzyme choline acetyltransferase (ChAT) is essential for ACh synthesis. To generate animals with a forebrain-restricted ablation of ACh production, we combined a conditional floxed allele of *ChAT* (*ChAT*$^{flox}$)[21] with an *Nkx2.1*$^{Cre}$ transgenic line in which cumulative recombination is restricted to the forebrain and hypothalamus[22] (Fig. 1a,b). Using an antisense cRNA probe directed against the floxed exons, we performed *in situ* hybridization for *ChAT* mRNA on cryosections prepared from non-mutant transgenic control (see Methods) and *ChAT* forebrain knock-out (*Nkx2.1*$^{Cre}$*; ChAT*$^{flox/flox}$; ‘forebrain KO’) brains at P30. These analyses revealed almost complete elimination of *ChAT* expression from

striatal cholinergic interneurons, with only 6 ± 3 *ChAT* positive cells in a representative set of forebrain KO striatal sections that spanned the rostrocaudal extent of the striatum (7 sections from each of 3 brains) *versus* 442 ± 18 *ChAT* positive cells in comparable sections from control brains (7 sections from each of 3 brains) (Fig. 1c,d). Similar efficacy of *ChAT* removal was also observed in the medial septum, diagonal band and nucleus basalis (Fig. 1e,f); cortical cholinergic interneurons were not affected since this $VIP^+$ population does not arise from an *Nkx2.1* expressing lineage[22]. Importantly, $Nkx2.1^{Cre}$ does not affect *ChAT* expression in the brainstem of $ChAT^{flox/flox}$ animals (Fig. 1g,h).

## Increased phasic-to-tonic DA release in forebrain ACh KO mice

We next examined the consequences of loss of forebrain cholinergic transmission on local DA release regulation using FCV to monitor evoked extracellular DA concentration ($[DA]_o$) in the dorsolateral region of the CPu in striatal slices. Release was evoked by either a single-pulse (1 p) stimulation that mimics one action potential or by brief five-pulse (5 p), phasic stimulation at varying frequencies. Consistent with previous pharmacological evidence that endogenous striatal ACh facilitates tonic DA release[13,14], peak $[DA]_o$ evoked by 1 p or by 5 p at low frequencies (≤10 Hz) was decreased in forebrain KO slices compared to control slices (Fig. 2a,b). However, peak $[DA]_o$ evoked by high frequency (100 Hz) stimulation was dramatically higher in the forebrain KO CPu (Fig. 2a,b). To establish whether the contrast between phasic-to-tonic DA release differed in control *versus* forebrain KO mice, we determined the ratio of 5 p evoked $[DA]_o$ to that evoked by 1 p at individual DA release sites; comparison of 5 p to 1 p ratios also normalized differences in absolute evoked $[DA]_o$ between recording sites. These data revealed a marked frequency dependence of DA release in the forebrain KO CPu that was absent in slices from control animals ($p<0.001$ at 25, 50 and 100 Hz in forebrain KO *versus* control, two-way ANOVA, Bonferroni correction, n=16–18 recording sites from 4–5 mice per group) (Fig. 2c). The pattern of increased frequency responsiveness of DA release mirrored that seen in control slices when nAChRs were blocked by mecamylamine (5 μM) or desensitized by nicotine (500 nM) (Fig. 2c). Moreover, in contrast to the effects seen in control slices, neither mecamylamine nor nicotine had a significant effect on $[DA]_o$ evoked by either tonic or phasic (>10 Hz) stimulation (Fig. 2c,d), demonstrating the complete absence of nAChR-dependent regulation of DA release in the CPu of forebrain KO animals.

Given differential regulation of DA release in dorsal and ventral striatum by ACh acting at nAChRs and muscarinic ACh receptors (mAChRs)[23–25], we examined patterns of evoked $[DA]_o$ in the NAc core and shell to address whether enhancement in phasic-to-tonic DA signaling in forebrain KO mice occurred throughout the dorsoventral extent of the striatal complex. Peak evoked $[DA]_o$ by 1 p was lower in NAc core and shell than in CPu in control mice, with CPu > NAc core > NAc shell ($p<0.001$ CPu *vs.* NAc shell, one-way ANOVA, Bonferroni correction, n=16 sites from 4 mice for CPu, n=9 sites from 3 mice for NAc core and shell). Also differing from CPu, both NAc core and shell exhibited bell-shaped frequency response curves with 5 p stimulation (Fig. 3), as reported previously[23,24,26,27]. Nevertheless, DA release evoked by 1 p or low-frequency 5 p stimulation was lower than in control mice in the NAc of forebrain KO mice (Fig. 3a,b,d,e). By contrast, release evoked by high frequency stimulation was enhanced in both NAc subregions of forebrain KO mice

(Fig. 3a,b,d,e), resulting in a marked amplification of phasic-to-tonic DA signaling at frequencies >10 Hz ($p<0.001$ at 25, 50 and 100 Hz in forebrain KO *versus* control, two-way ANOVA, Bonferroni correction, n=9–14 recording sites from 3 mice per group) (Fig. 3a,c,d,f). These data confirm the loss of DA release regulation by endogenous ACh throughout the striatal complex of forebrain KO mice.

## Generation of brainstem and double forebrain/brainstem ACh KO mice

Using a similar genetic approach to that used to produce forebrain *ChAT* KO mice, we generated rostral brainstem *ChAT* KO animals using the $En1^{Cre}$ driver[28], whose cumulative recombination is restricted to the mes/r1 embryonic territory (Fig. 4a,b), and as such, primarily affects the PTg and LDTg but not brainstem motor nuclei that arise from more caudal regions (e.g., Mo5) (Fig. 4c,d,g). *ChAT* brainstem KO mice ($En1^{Cre}$; $ChAT^{flox/flox}$; 'brainstem KO') had no *ChAT*-positive cells remaining in the rostral brainstem as determined by *in situ* hybridization in a representative set of sections, whereas control mice had 234 ± 10 *ChAT*-positive cells in comparable fields (n=3 brains for each genotype, 5 comparable sections spanning the PTg/LDTg region counted per brain) (Fig. 4c,d). Demonstrating the regional segregation of this ablation strategy, striatal *ChAT* expression in brainstem KO mice did not differ from that in control mice (Fig. 4e,f). We then combined these two conditional KO strategies and generated forebrain/brainstem ACh double knock-out ('double KO') mice.

## Striatal DA release in brainstem and double ACh KO mice

To confirm that local cholinergic regulation of striatal DA was functionally intact in brainstem KO mice, we examined the frequency dependence of evoked DA release in striatal slices from these animals. Patterns of 1 p and 5 p evoked $[DA]_o$ in the CPu of these animals did not differ from those in control mice (Fig. 5a,b), and were as sensitive as controls to nAChR antagonism by mecamylamine or by nicotine-induced desensitization (Fig. 5c,d). These *in vitro* data demonstrate that there is no alteration in local cholinergic regulation of striatal DA release or other compensatory changes in response to the chronic loss of brainstem ACh. We then examined DA release in striatal slices from double KO mice. As in forebrain KO mice, 1 p evoked $[DA]_o$ in the CPu was lower in double KO *versus* control mice with enhanced phasic-to-tonic DA release, and concomitant loss of effect of mecamylamine and nicotine on evoked $[DA]_o$ (Fig. 5). These data confirm the functional loss of forebrain ACh in double KO mice, as seen in forebrain KO mice. Of course, in these *in vitro* experiments the pattern of stimulation is experimenter driven, whereas *in vivo* the pattern will be determined by DA neuron firing activity that then undergirds striatal DA release[29] and its consequent influence on motor behavior.

## Differential locomotor behavior of ACh KO mice in a novel environment

To test the behavioral consequences arising from the total loss of forebrain and or brainstem cholinergic regulation, we evaluated the locomotor behavior of naive mice in the novel environment of the open field arena, which is linked to burst firing of DA neurons and consequent DA release [19,20,30,31]. Forebrain KO mice were hyperactive and hyperkinetic, in that the total distance traveled during the first 10 min in the arena was significantly greater than non-mutant littermate control mice (Fig. 6a), and movement velocity was enhanced

(Fig. 6b). To assess the DA dependence of open field activity, we administered the competitive D2 receptor antagonist raclopride, the displacement of which is commonly used as an index of dopamine release in human PET studies[32,33]. We found that raclopride was effective at suppressing total locomotor activity in forebrain KO mice, but only at a higher dose (>0.25 mg/kg) than that necessary to decrease activity in control mice (Fig. 6d). The decreased efficacy of low-dose raclopride in forebrain KO mice argues against a role for increased receptor sensitivity from decreased tonic DA release as a contributing factor in the motor response. Instead, these data indicate elevated $[DA]_o$ at postsynaptic D2 receptors on striatal output neurons in these animals when placed in a novel environment, and are consistent with the increase in phasic *versus* tonic striatal DA efflux observed in response to phasic stimulation *in vitro* (Fig. 2, Fig. 3).

Considering that brainstem cholinergic inputs regulate the transition of midbrain DA neurons from tonic to burst firing modes[9], we next examined the effects of removing these brainstem ACh signaling pathways on exploratory behavior in the novel environment of the open field arena (Fig. 6). Brainstem KO animals exhibited significantly less exploratory activity in the open field, and were hypokinetic compared to control mice (Fig. 6a,b). Because the removal of *ChAT* was restricted to the rostral brainstem, this hypoactivity was not due to loss of cholinergic activity from motor neurons in the hindbrain or spinal cord (Fig. 4c,d,g). These data are consistent with the expected decrease in phasic DA neuron firing with loss of brainstem cholinergic input. Indeed, raclopride had little effect on exploratory motor activity, even at the higher dose (Fig. 6d), thereby suggesting lower burst-driven D2 receptor activation in these animals than in control mice. Remarkably, the exploratory activity of animals lacking both forebrain- and brainstem-derived ACh was normalized to that of non-mutant control mice (mean distance traveled, $p>0.05$ *vs.* control) (Fig. 6a), as was the velocity of movement ($p>0.05$ *vs.* control) (Fig. 6b). Thus, the enhanced phasic-to-tonic striatal DA release in these mice can compensate for the diminished burst output of midbrain DA neurons arising from the loss of brainstem cholinergic signaling, resulting in normal motor output. Consistent with a key role for burst-driven D2 receptor activation during exploration of a novel environment, double KO mice showed similar insensitivity to raclopride to that seen in brainstem KO animals (Fig. 6d). We did not find any difference across genotypes in the ratio of time spent in the center *versus* perimeter zones of the open field arena during the 10 min of testing (Fig. 6c), indicating that anxiety-related behavior changes were not a contributing factor to the differences in exploration observed across the genotypes.

## Discussion

We show here that loss of forebrain ACh leads to increased phasic-to-tonic DA signaling throughout the striatal complex and hyperactivity in contexts that stimulate brainstem ACh activity and burst firing of DA neurons (e.g., a novel environment), whereas loss of brainstem ACh leads to hypoactivity under similar conditions. Nevertheless, the striatum does not work in isolation, so that it is likely that the behavior observed in our forebrain KOs is a synthetic phenotype arising from the total removal of forebrain ACh, with consequent alterations in the activities of descending glutamatergic projections from the prefrontal cortex, ventral pallidum, and hippocampus that converge upon the SNc/VTA. Overall, our

results support a model in which brainstem cholinergic inputs to midbrain DA neurons provide key regulation of the transition from tonic to burst firing modes that is then stimulated by diverse glutamatergic inputs[34], with independent regulation of axonal DA release probability in the striatum by cholinergic interneurons signaling through nAChRs (Fig. 6e).

A number of studies have examined the role of forebrain cholinergic neurons (striatal and projection) in regulating motor activity; however, to date the overall conclusion remains unclear. Complete loss of cholinergic cells in the NAc leads to hyperactivity[35], whereas disruption of ACh neurotransmission via genetic ablation of the vesicular ACh transporter (*VAChT*) in all striatal interneurons does not change spontaneous locomotor activity[36]. Given that striatal cholinergic interneurons can co-release glutamate[37], Guzman and colleagues argue that the lack of change in locomotor activity is because glutamate release remains intact in this *VAChT* KO model. On the other hand, optogenetic inhibition of cholinergic interneurons in the CPu or NAc, which should prevent release of both ACh and glutamate, also has no effect on spontaneous locomotor behavior[38,39]. It is relevant to note that immunolesions of forebrain cholinergic projection neurons with 192 IgG-saporin (which spares striatal cholinergic interneurons) also fail to produce alterations in locomotion behavior[40].

Our studies differ from this previous body of work in several ways. First by targeting ChAT we examined the complete and selective loss of ACh, whereas disruption of VAChT leads to the accumulation of intracellular ACh[41] that could potentially result in residual cholinergic tone via non-quantal release mediated by the choline transporter[42]. Second, we deliberately examined motor behavior in a novel environment, which leads to DA neuron burst firing and consequent DA release[19,20,30,31]. This novelty is lost in typical studies of locomotor behavior that include an acclimation step[43]. Our data therefore refocus attention back on cholinergic regulation of striatal DA release as a component of motivated behavior. The importance of these behavioral findings has been augmented by the recent demonstration that activation of striatal cholinergic interneurons directly triggers axonal DA release[11,12]. Our results in forebrain KO mice indicate that in the absence of local DA release regulation by striatal ACh in forebrain *ChAT* KO mice, the consequent absence of cholinergic gating of DA release leads to DA signaling that more faithfully reflects DA neuron activity.

The simplest explanation for the hypoactive phenotype of brainstem KO mice is decreased phasic activity of midbrain DA neurons[9]; however, other structures also receive cholinergic innervation from the PTg and LDTg, including the thalamus[44]. Given that the thalamus provides glutamatergic inputs to MSNs, reduction of cholinergic signaling within the thalamus could be a contributing factor to the hypoactivity phenotype observed. However, since thalamic input provides much less robust excitation of MSNs than does cortical input[45], changes in thalamic activation alone should have only a minor direct effect on MSN output. Glutamatergic input from the thalamus can also activate striatal cholinergic interneurons[11,46], although the net consequence of this on motor behavior is difficult to predict. Thalamic activation can trigger striatal DA release via stimulation of local cholinergic interneurons and consequent activation of nAChRs on DA axons[11,46], such that removal of brainstem cholinergic input to the thalamus could contribute to the hypoactivity

seen in brainstem ACh KO mice via reduction of this pathway. On the other hand, thalamic activation of cholinergic interneurons can also decrease glutamatergic input to MSNs via mAChRs on cortical and thalamic terminals[46,47], and enhance activation of indirect-pathway MSNs[15,46,48], so that reduction of this process would be predicted to contribute to hyperactivity, which is opposite from what we observed in brainstem ACh KO mice.

In addition to the thalamus, loss of brainstem cholinergic input to other brain regions might also contribute to the observed hypoactivity phenotype. General PTg lesion does lead to hypoactivity and to increased activity of the subthalamic nucleus (STN) and SN pars reticulata (SNr); however, these responses are thought to be secondary to the glutamatergic PTg inputs to SNc DA neurons[49] that would not be affected by brainstem *ChAT* removal. Strikingly, motor behavior is normal in double KO mice, suggesting that any deficits in DA neuron burst firing from loss of brainstem cholinergic inputs is compensated by amplification of striatal phasic-to-tonic DA signaling in the absence of local cholinergic regulation[11]. Behavioral normalization in double KOs also argues against a primary role for thalamic drive of cholinergic interneurons and consequent DA release in exploratory behavior in a novel environment.

The mice introduced here provide unique models in which to examine the role of ACh in a variety of behavioral contexts. Indeed, a major advantage of these mice is that they provide a reproducible and non-invasive means of selectively eliminating cholinergic activity in forebrain *versus* brainstem regions without loss of the cells themselves. This is important given that many of these neurons can also release other transmitters/modulators in addition to ACh that may impact brain physiology[37]. Thus, the selective removal of ACh synthesis achieved by our genetic methods provides a more specific means by which to examine the role of ACh in brain function and animal behavior.

The present findings highlight the critical role of forebrain and brainstem cholinergic signaling in regulating exploratory motor activity, and how imbalances in brain cholinergic tone can affect pathways that converge on dopaminergic circuits. The distinct differences in DA-dependent behaviors between forebrain and brainstem ACh KO mice and the normalization of motor behavior in double KOs provides novel insights into ACh/DA interactions and the balance of ACh activities throughout the brain that is required for proper motor function.

## Methods

### Mice and genotyping

Mice harboring a conditional (‘floxed’) allele for *ChAT* were obtained as a kind gift from Dr. Joshua Sanes[21]. Genotyping by PCR for the wild-type *ChAT* allele was performed with the following primers: 5′-CAACCGCCTGGCCCTGCCAGTCAACTCTAG-3′ and 5′-GAGGATGAAATCCTGACAGATTCCAACAGG-3′. The $ChAT^{flox}$ allele was genotyped by PCR using the following primers: 5′-TGGTTCTTTCCGCCTCAGGACTCTTCCTTT-3′ and 5′-TAACCAAACGTAATATATGTTTGTTGGAGC-3′. The $Nkx2.1^{Cre}$ BAC transgenic line[22], a kind gift from Dr. Stewart Anderson, was genotyped using the primers 5′-AAGGCGGACTCGGTCCACTCCG-3′ and 5′-TCGGATCCGCCGCATAACCAG-3′. The

*En1*$^{Cre}$ line[28], a kind gift from Dr. Alex Joyner, was genotyped using the primers 5′-GCCTTCTTCCTCTCCGCGCAC-3′ and 5′-TCGGATCCGCCGCATAACCAG-3′ (same reverse *Cre* primer as used with *Nkx2.1*$^{Cre}$ genotyping).

All experiments used heterozygous non-mutant transgenic littermates as controls (i.e., *Nkx2.1*$^{Cre}$*; ChAT*$^{flox/+}$, *En1*$^{Cre}$*; ChAT*$^{flox/+}$, *ChAT*$^{flox/flox}$ and *ChAT*$^{flox/+}$ are referred to as 'control' in the main text). We used these littermate controls rather than genuine wild-type (*ChAT*$^{+/+}$) animals to subtract out non-specific phenotypes that might arise from the presence of the *Cre* allele (e.g., non-specific effects of Cre recombinase expression, or genomic alterations arising from transgene insertion) or *ChAT*$^{flox}$ allele (e.g., potentially hypomorphic properties). It should be noted, however, that the expression pattern of *ChAT* mRNA as determined by *in situ* hybridization staining did not differ among the control genotypes. Moreover, levels of ACh should not be altered in these heterozygous control animals, as although ChAT enzymatic activity is essential for ACh production it is not the rate-limiting step, which is consistent with a lack of differences in voltammetric or behavioral data among these control groups.

All animal handling procedures were in accordance with National Institutes of Health guidelines and were approved by the Institutional Animal Care and Use Committees of New York University School of Medicine.

## In situ hybridization

To generate an antisense cRNA *in situ* hybridization probe specific for the region flanked by loxP sites (exons 3–4), the following primers were used to generate a PCR template for probe synthesis (T7) from a full length mouse *ChAT* cDNA clone (Open Biosystems clone ID: 40129512): 5′-GACTTACCTAAGTTGCCAGTG-3′ and 5′-AATTAATACGACTCACTATAGCTTAGCTGGTCATTGGTGT-3′. *In situ* hybridization with digoxigenin – labeled cRNA probes was performed essentially as previously described[50]. Briefly, sections (16–20 μm thick) were air dried, fixed in 4% paraformaldehyde in phosphate buffered saline (PBS), pH 7.2 (PFA; 10 minutes at 4°C), treated at room temperature sequentially with 1.5% $H_2O_2$ in methanol (15 minutes), 0.2M HCl (8 minutes), proteinase K (10 μg/mL PBS; 5 minutes), 4% PFA (10 minutes, 4°C), and acetylation buffer (0.1M triethanolamine, 0.045N NaOH, 0.025% acetic anhydride), with PBS washes (3× 5 minutes) between each step, prior to overnight hybridization at 55°C (100 ng probe/mL buffer: 50% formamide, 10% dextran sulfate, 1% Denhardt's solution, 250 μg/mL yeast tRNA, 0.3M NaCl, 20 mM Tris-HCl pH 8.0, 5 mM EDTA, 10 mM $NaH_2PO_4$, 1% sarcosyl). Following hybridization, slides were washed in saline-sodium citrate buffer (SSC)/50% formamide at 65°C, treated with RNase (20 μg/mL in 0.5M NaCl, 10 mM Tris-HCl, pH 7.5, 5 mM EDTA), and incubated overnight with anti-digoxigenin Fab fragments conjugated to peroxidase (Roche; 1:500 dilution in 100 mM maleic acid, 150 mM NaCl, 0.05% Tween-20, pH 7.5, with 1% blocking reagent). Following sequential incubations with biotinyl-tyramide and streptavidin-alkaline phosphatase, signal was visualized with standard nitro-blue tetrazolium (NBT) and 5-bromo-4-chloro-3′-indolyl phosphate (BCIP) histochemistry. Hybridized sections were counterstained with Fast Red (Vector Labs),

dehydrated, and coverslipped with Permount prior to imaging with a Zeiss Axioplan brightfield microscope.

### Voltammetric recording of DA release in striatal slices

Procedures for preparing striatal slices and voltammetric recording of striatal DA release were according to those described previously[13,51–53]. Coronal forebrain slices (350 μm thick) were prepared from transgenic mice and their non-mutant control littermates (3 to 5 months of age) using a VT200S vibrating blade microtome (Leica Microsystems), then maintained in HEPES-buffered artificial cerebrospinal fluid (aCSF) at room temperature for at least 1 h before experimentation. Male mice were used for recordings in CPu whereas females were used for measurements in the nucleus accumbens (NAc).

For recording, slices were transferred to a submersion chamber (Warner Instruments LLC) maintained at 32 °C and superfused at 1.2 mL/min with bicarbonate-buffered aCSF containing (in mM): NaCl (124); KCl (3.7); $NaHCO_3$ (26); $MgSO_4$ (1.3); $KH_2PO_4$ (1.3); glucose (10); $CaCl_2$ (2.4) and saturated with 95% $O_2$/5% $CO_2$. After an equilibration period of at least 30 min, fast-scan cyclic voltammetry with carbon-fiber microelectrodes (7 μm diameter, 30 to 70 μm length, manufactured in-house) was used to monitor evoked $[DA]_o$. Release of DA was elicited in either the dorsolateral portion of the striatum, the NAc core or the NAc shell using concentric bipolar stimulating electrodes placed on the surface of the slice ventromedially to the carbon fiber recording electrode.

Voltammetric measurements were made using a Millar voltammeter (available by special request to Dr. Julian Millar at St. Bartholomew's and the Royal London School of Medicine and Dentistry, University of London, UK). Scan range was −0.7 V to +1.3 V (*vs.* Ag/AgCl), scan rate was 800 V/s, and the sampling interval was 100 ms. Data were acquired using a DigiData 200B A/D board controlled by Clampex 7.0 software (Molecular Devices). Released DA was identified according to voltammograms showing the single oxidation and reduction peak potentials that characterize the voltammetric signature of DA. To quantify evoked $[DA]_o$, electrodes were calibrated with known concentrations of DA at 32 °C after each experiment in aCSF in the presence and absence of each drug used during a given experiment.

To decrease recording bias, the experimental design for the CPu typically involved sampling $[DA]_o$ in 4 recording sites of each striatal slice; 2 sites in control conditions and 2 sites in either mecamylamine (5 μM, Sigma) or nicotine (500 nM, Sigma). Two slices (one for each drug) were examined per mouse during an experimental day. In each recording site, release of DA was evoked by single pulse (1 p) stimulation (0.4 to 0.6 mA amplitude, 0.1 ms duration) and by stimulation with five pulses (5 p) at 5, 10, 25, 50 and 100 Hz, applied at 5 min intervals. Stimulation frequencies were presented in either an ascending or descending order in the first control recording site and reversed for the second control site. The drug (either mecamylamine or nicotine) was then applied to the superfusing aCSF for at least 10 to 15 min before these patterns of stimulation were repeated for recording sites in the presence of drug. Experiments in the NAc core and shell were conducted in a similar manner to those described for the CPu only with 2 to 4 recording sites sampled in each NAc sub-region of a single coronal slice in the absence of drugs.

### Open field behavioral assays

Open field video recordings were performed in a 40×40cm white plexiglass arena using Noldus Ethovision Pro 3.1 tracking and analysis software. Naive experimental and control littermate male and female mice between 6–10 weeks of age were transferred in their respective home cages to the testing room at least 30 minutes prior to being placed in the clean arena. The first 10 minutes of activity were recorded for each mouse. We excluded one forebrain KO animal from the statistical analysis due to extreme hyperactivity. Raclopride (Sigma) in PBS was administered at the doses indicated by intraperitoneal injection 15 minutes prior to recording of animals in the open field arena.

### Data Analysis

Voltammetric DA recording: data are expressed as mean ± SEM where *n* indicates the number of recording sites in 1 to 3 slices from 3 to 5 mice per group and illustrated as either absolute $[DA]_o$ or the ratio of 5 p evoked $[DA]_o$ to 1 p. Open field activity recordings: data are expressed as mean ± SEM, where *n* indicates the number of mice, and illustrated as total distance traveled and velocity of movement. Data were analyzed using GraphPad Prism Software. Significance of differences was assessed using either an unpaired t-test, one-way ANOVA or two-way ANOVA as appropriate. Significance was considered to be $p<0.05$.

## Acknowledgments

This work was supported by Alzheimer's Association grant 90664 (R.P.M.; awarded to Dr. B. Rudy), NIH R01 grant MH068469 (R.P.M.; awarded to Dr. G. Fishell), FRSQ training award (E.R.), NIH/NINDS R01 grant NS036362 (M.E.R.) and the Attilio and Olympia Ricciardi Research Fund (M.E.R.).

## References

1. Redgrave P, Gurney K, Reynolds J. What is reinforced by phasic dopamine signals? Brain Res Rev. 2008; 58:322–339. [PubMed: 18055018]
2. Gerfen CR, Surmeier DJ. Modulation of striatal projection systems by dopamine. Annu Rev Neurosci. 2011; 34:441–466. [PubMed: 21469956]
3. Schultz W. Potential vulnerabilities of neuronal reward, risk, and decision mechanisms to addictive drugs. Neuron. 2011; 69:603–617. [PubMed: 21338874]
4. Lester DB, Rogers TD, Blaha CD. Acetylcholine-dopamine interactions in the pathophysiology and treatment of CNS disorders. CNS Neurosci Ther. 2010; 16:137–162. [PubMed: 20370804]
5. Grenhoff J, Aston-Jones G, Svensson TH. Nicotinic effects on the firing pattern of midbrain dopamine neurons. Acta Physiol Scand. 1986; 128:351–358. [PubMed: 3788613]
6. Floresco SB, West AR, Ash B, Moore H, Grace AA. Afferent modulation of dopamine neuron firing differentially regulates tonic and phasic dopamine transmission. Nature Neurosci. 2003; 6:968–973. [PubMed: 12897785]
7. Mena-Segovia J, Winn P, Bolam JP. Cholinergic modulation of midbrain dopaminergic systems. Brain Res Rev. 2008; 58:265–71. [PubMed: 18343506]
8. Drenan RM, et al. In vivo activation of midbrain dopamine neurons via sensitized, high-affinity alpha 6 nicotinic acetylcholine receptors. Neuron. 2008; 60:123–136. [PubMed: 18940593]
9. Lodge DJ, Grace AA. The laterodorsal tegmentum is essential for burst firing of ventral tegmental area dopamine neurons. Proc Natl Acad Sci U S A. 2006; 103:5167–5172. [PubMed: 16549786]
10. Zhou FM, Liang Y, Dani JA. Endogenous nicotinic cholinergic activity regulates dopamine release in the striatum. Nature Neurosci. 2001; 4:1224–1229. [PubMed: 11713470]
11. Threlfell S, et al. Striatal dopamine release is triggered by synchronous activity in cholinergic interneurons. Neuron. 2012; 75:58–64. [PubMed: 22794260]

12. Cachope R, et al. Selective activation of cholinergic interneurons enhances accumbal phasic dopamine release: setting the tone for reward processing. Cell Reports. 2012; 2:1–9. [PubMed: 22840390]
13. Rice ME, Cragg SJ. Nicotine amplifies reward-related dopamine signals in striatum. Nature Neurosci. 2004; 7:583–584. [PubMed: 15146188]
14. Zhang H, Sulzer D. Frequency-dependent modulation of dopamine release by nicotine. Nature Neurosci. 2004; 7:581–582. [PubMed: 15146187]
15. Oldenburg IA, Ding JB. Cholinergic modulation of synaptic integration and dendritic excitability in the striatum. Curr Opin Neurobiol. 2011; 21:425–432. [PubMed: 21550798]
16. Wang JQ, McGinty JF. Intrastriatal injection of a muscarinic receptor agonist and antagonist regulates striatal neuropeptide mRNA expression in normal and amphetamine-treated rats. Brain Res. 1997; 748:62–70. [PubMed: 9067445]
17. Grace AA, Floresco SB, Goto Y, Lodge DJ. Regulation of firing of dopaminergic neurons and control of goal-directed behaviors. Trends Neurosci. 2007; 30:220–227. [PubMed: 17400299]
18. Morikawa H, Paladini CA. Dynamic regulation of midbrain dopamine neuron activity: intrinsic, synaptic, and plasticity mechanisms. Neuroscience. 2011; 198:95–111. [PubMed: 21872647]
19. Giros B, Jaber M, Jones SR, Wightman RM, Caron MG. Hyperlocomotion and indifference to cocaine and amphetamine in mice lacking the dopamine transporter. Nature. 1996; 379:606–6120. [PubMed: 8628395]
20. Gainetdinov RR, et al. Role of serotonin in the paradoxical calming effect of psychostimulants on hyperactivity. Science. 1999; 283:397–401. [PubMed: 9888856]
21. Misgeld T, et al. Roles of neurotransmitter in synapse formation: development of neuromuscular junctions lacking choline acetyltransferase. Neuron. 2002; 36:635–648. [PubMed: 12441053]
22. Xu Q, Tam M, Anderson SA. Fate mapping Nkx2.1-lineage cells in the mouse telencephalon. J Comp Neurol. 2008; 506:16–29. [PubMed: 17990269]
23. Zhang T, et al. Dopamine signaling differences in the nucleus accumbens and dorsal striatum exploited by nicotine. J Neurosci. 2009; 29:4035–4043. [PubMed: 19339599]
24. Threlfell S, et al. Striatal muscarinic receptors promote activity dependence of dopamine transmission via distinct receptor subtypes on cholinergic interneurons in ventral versus dorsal striatum. J Neurosci. 2010; 30:3398–3408. [PubMed: 20203199]
25. Exley R, McIntosh JM, Marks MJ, Maskos U, Cragg SJ. Striatal α5 nicotinic receptor subunit regulates dopamine transmission in dorsal striatum. J Neurosci. 2012; 32:2352–2356. [PubMed: 22396410]
26. Patel J, Trout SJ, Kruk ZL. Regional differences in evoked dopamine efflux in brain slices of rat anterior and posterior caudate putamen. Naunyn Schmiedebergs Arch Pharmacol. 1992; 346:267–276. [PubMed: 1407013]
27. Trout SJ, Kruk ZL. Differences in evoked dopamine efflux in rat caudate putamen, nucleus accumbens and tuberculum olfactorium in the absence of uptake inhibition: influence of autoreceptors. Brit J Pharmacol. 1992; 106:452–458. [PubMed: 1393270]
28. Kimmel RA, et al. Two lineage boundaries coordinate vertebrate apical ectodermal ridge formation. Genes Dev. 2000; 14:1377–1389. [PubMed: 10837030]
29. Sombers LA, Beyene M, Carelli RM, Wightman RM. Synaptic overflow of dopamine in the nucleus accumbens arises from neuronal activity in the ventral tegmental area. J Neurosci. 2009; 29:1735–1742. [PubMed: 19211880]
30. Rebec GV, Grabner CP, Johnson M, Pierce RC, Bardo MT. Transient increases in catecholaminergic activity in medial prefrontal cortex and nucleus accumbens shell during novelty. Neuroscience. 1997; 76:707–714. [PubMed: 9135044]
31. Marinelli M, White FJ. Enhanced vulnerability to cocaine self-administration is associated with elevated impulse activity of midbrain dopamine neurons. J Neurosci. 2000; 20:8876–8885. [PubMed: 11102497]
32. Koepp MJ, et al. Evidence for striatal dopamine release during a video game. Nature. 1998; 393:266–268. [PubMed: 9607763]
33. Egerton A, et al. The dopaminergic basis of human behaviors: A review of molecular imaging studies. Neurosci Biobehav Rev. 2009; 33:1109–1132. [PubMed: 19481108]

34. Watabe-Uchida M, Zhu L, Ogawa SK, Vamanrao A, Uchida N. Whole-brain mapping of direct inputs to midbrain dopamine neurons. Neuron. 2012; 74:858–873. [PubMed: 22681690]
35. Kaneko S, et al. Synaptic integration mediated by striatal cholinergic interneurons in basal ganglia function. Science. 2000; 289:633–637. [PubMed: 10915629]
36. Guzman MS, et al. Elimination of the vesicular acetylcholine transporter in the striatum reveals regulation of behaviour by cholinergic-glutamatergic co-transmission. PLoS Biol. 2011; 9:e1001194. [PubMed: 22087075]
37. Higley MJ, et al. Cholinergic interneurons mediate fast VGluT3-dependent glutamatergic transmission in the striatum. PLoS One. 2011; 6:e19155. [PubMed: 21544206]
38. Witten IB, et al. Cholinergic interneurons control local circuit activity and cocaine conditioning. Science. 2010; 330:1677–1681. [PubMed: 21164015]
39. English DF, et al. GABAergic circuits mediate the reinforcement-related signals of striatal cholinergic interneurons. Nature Neurosci. 2012; 15:123–130.
40. Leanza G, Nilsson OG, Nikkhah G, Wiley RG, Bjorklund A. Effects of neonatal lesions of the basal forebrain cholinergic system by 192 immunoglobulin G-saporin: biochemical, behavioural and morphological characterization. Neuroscience. 1996; 74:119–141. [PubMed: 8843082]
41. Martins-Silva C, et al. Novel strains of mice deficient for the vesicular acetylcholine transporter: insights on transcriptional regulation and control of locomotor behavior. PLoS One. 2011; 6:e17611. [PubMed: 21423695]
42. Chavez J, Vargas MH, Cruz-Valderrama JE, Montano LM. Non-quantal release of acetylcholine in guinea-pig airways: role of choline transporter. Exp Physiol. 2011; 96:460–467. [PubMed: 21278079]
43. Pierce RC, Kalivas PW. Locomotor behavior. Curr Protoc Neurosci. 2007; Chapter 8
44. Hallanger AE, Levey AI, Lee HJ, Rye DB, Wainer BH. The origins of cholinergic and other subcortical afferents to the thalamus in the rat. J Comp Neurol. 1987; 262:105–124. [PubMed: 2442206]
45. Ding J, Peterson JD, Surmeier DJ. Corticostriatal and thalamostriatal synapses have distinctive properties. J Neurosci. 2008; 28:6483–6492. [PubMed: 18562619]
46. Ding JB, Guzman JN, Peterson JD, Goldberg JA, Surmeier DJ. Thalamic gating of corticostriatal signaling by cholinergic interneurons. Neuron. 2010; 67:294–307. [PubMed: 20670836]
47. Pakhotin P, Bracci E. Cholinergic interneurons control the excitatory input to the striatum. J Neurosci. 2007; 27:391–400. [PubMed: 17215400]
48. Shen W, et al. Cholinergic modulation of Kir2 channels selectively elevates dendritic excitability in striatopallidal neurons. Nature Neurosci. 2007; 10:1458–1466. [PubMed: 17906621]
49. Breit S, Lessmann L, Benazzouz A, Schulz JB. Unilateral lesion of the pedunculopontine nucleus induces hyperactivity in the subthalamic nucleus and substantia nigra in the rat. Eur J Neurosci. 2005; 22:2283–2294. [PubMed: 16262666]
50. Batista-Brito R, Machold R, Klein C, Fishell G. Gene expression in cortical interneuron precursors is prescient of their mature function. Cereb Cortex. 2008; 18:2306–2317. [PubMed: 18250082]
51. Patel JC, Witkovsky P, Avshalumov MV, Rice ME. Mobilization of calcium from intracellular stores facilitates somatodendritic dopamine release. J Neurosci. 2009; 29:6568–6579. [PubMed: 19458227]
52. Bao L, Patel JC, Walker RH, Shashidharan P, Rice ME. Dysregulation of striatal dopamine release in a mouse model of dystonia. J Neurochem. 2010; 114:1781–1791. [PubMed: 20626557]
53. Patel JC, Rice ME. Monitoring axonal and somatodendritic dopamine release using fast-scan cyclic voltammetry in slices. Methods Mol Biol. 2013; 964:243–273. [PubMed: 23296788]

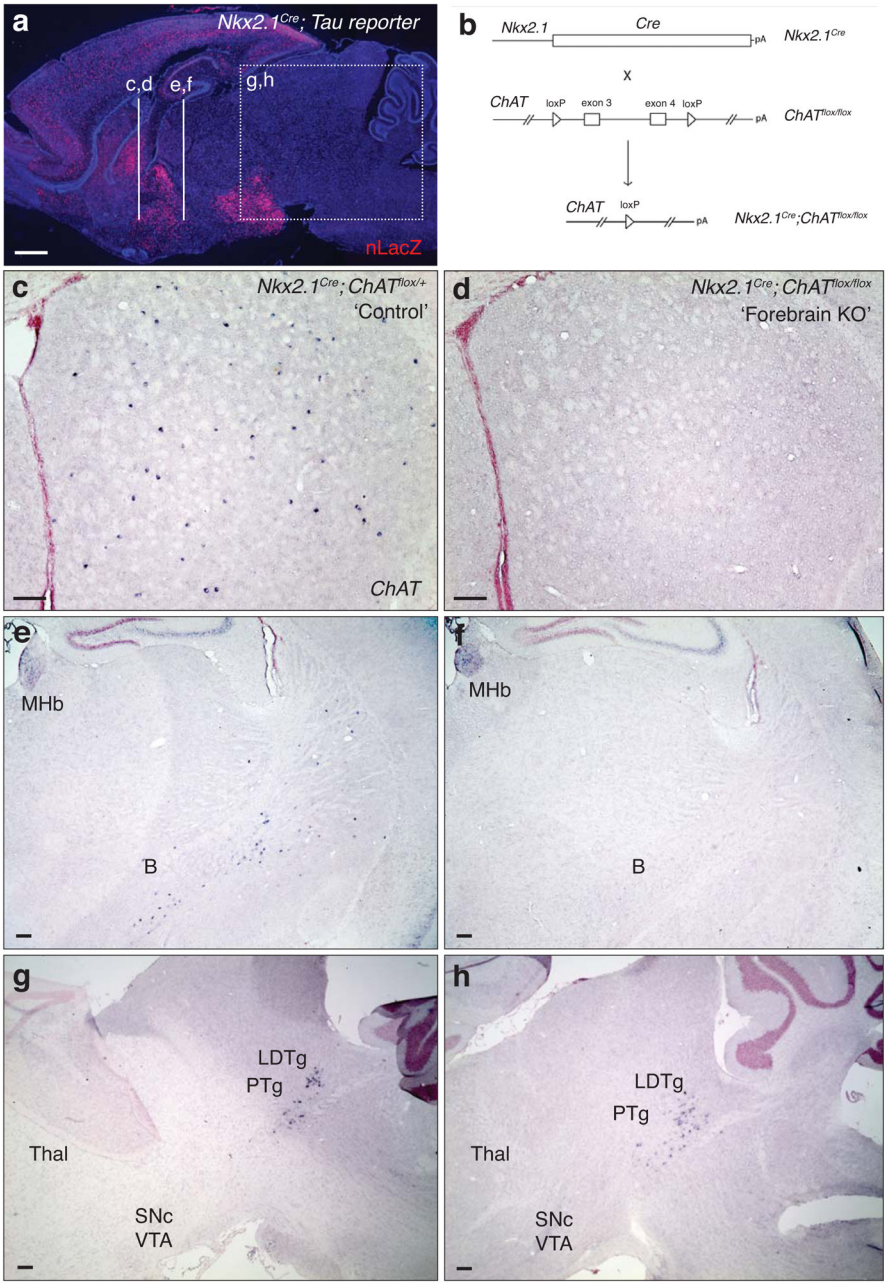


**Figure 1.**

Genetic strategies for targeted ablation of ACh production in the forebrain (**a**) Sagittal field of a P21 *Nkx2.1*$^{Cre}$*; Tau*$^{loxP\text{-}stop\text{-}loxP\text{-}mGFPiresNLSLacZ}$ (‘*Tau reporter*’) mouse brain illustrating the populations (nLacZ$^{+}$; red) that arise from *Nkx2.*1 expressing lineages. (**b**) Genetic strategy for selective elimination of ACh production within the forebrain (*Nkx2.1* lineages). (**c–d**) *In situ* hybridization for *ChAT* mRNA in coronal striatal brain cryosections from *Nkx2.1*$^{Cre}$*; ChAT*$^{flox/+}$ non-mutant control (**c**) and *Nkx2.1*$^{Cre}$*; ChAT*$^{flox/flox}$ forebrain KO (**d**) mice at P30 revealed a complete loss of *ChAT* expression in the striatum of the forebrain KO. (**e–f**) Coronal fields of control (*Nkx2.1*$^{Cre}$*; ChAT*$^{flox/+}$; **e**) and mutant

('forebrain KO'; *Nkx2.1*$^{Cre}$*; ChAT*$^{flox/flox}$; **f**) P30 brain sections stained by *in situ* hybridization for *ChAT* mRNA illustrate the removal of *ChAT* expression within the nucleus basalis, in addition to the striatum (**c,d**) and other ventral forebrain cholinergic populations. (**g–h**) *ChAT* expression within the rostral brainstem (e.g., PTg, LDTg) is not affected in the forebrain KO. MHb, medial habenular nu; B, nu basalis of Meynert; Thal, thalamus; PTg, pedunculopontine nucleus; LDTg, laterodorsal tegmental nucleus; SNc, substantia nigra pars compacta; VTA, ventral tegmental area. Scale bar in (**a**) represents 1 mM; scale bars in (**c–h**) represent 300 μM.

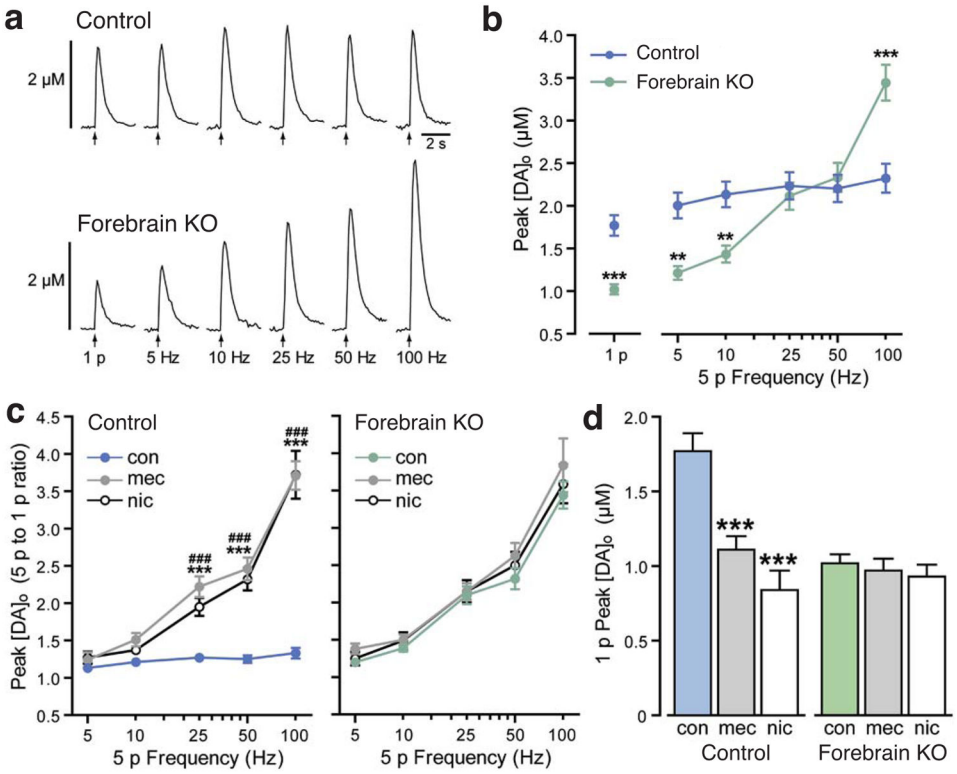


**Figure 2.**

Loss of forebrain ACh production results in enhanced phasic-to-tonic DA signaling within the dorsal striatum. (**a–d**) Voltammetric monitoring of extracellular DA concentration ($[DA]_o$) in the caudate putamen (CPu) of striatal slices. (**a**) Representative single-pulse (1 p) and five-pulse (5 p) evoked $[DA]_o$ recorded in control and forebrain KO mice. (**b**) Mean peak $[DA]_o$ evoked by 1 p and 5 p stimulation in each group shows suppression of DA release up to 10 Hz, maintenance of release levels at 25 and 50 Hz, and enhanced peak $[DA]_o$ at 100 Hz (**p<0.01; ***p<0.001 *vs.* control; unpaired t-test for comparison of 1 p or two-way ANOVA with Bonferroni correction for comparison of 5 p). (**c**) Frequency dependence (5 p to 1 p ratio) of evoked $[DA]_o$ in control and forebrain KO mice under control conditions (con) and in the presence of the nAChR antagonist mecamylamine (mec, 5 μM) or a desensitizing concentration of nicotine (nic, 500 nM) (***p<0.001 mec *vs.* con, $^{###}$p<0.001 nic *vs.* con, two-way ANOVA with Bonferroni correction). The 1 p-to-5 p ratios in forebrain KO mice under control conditions were indistinguishable from those in control mice in mec or nic (p>0.05 for each frequency for either mec or nic, two-way ANOVA with Bonferroni correction). (**d**) 1 p evoked $[DA]_o$ in forebrain KO mice, unlike in control mice, was not suppressed by either mec or nic (***p<0.001 *vs.* con, one-way ANOVA with Dunnett's correction). Control data are from 4 mice with n=16 recording sites in control conditions and n=8 sites in each drug. Data for forebrain KOs are from 5 mice with n=18 recording sites in control conditions and n=9 sites in each drug. All data are means ± SEM.

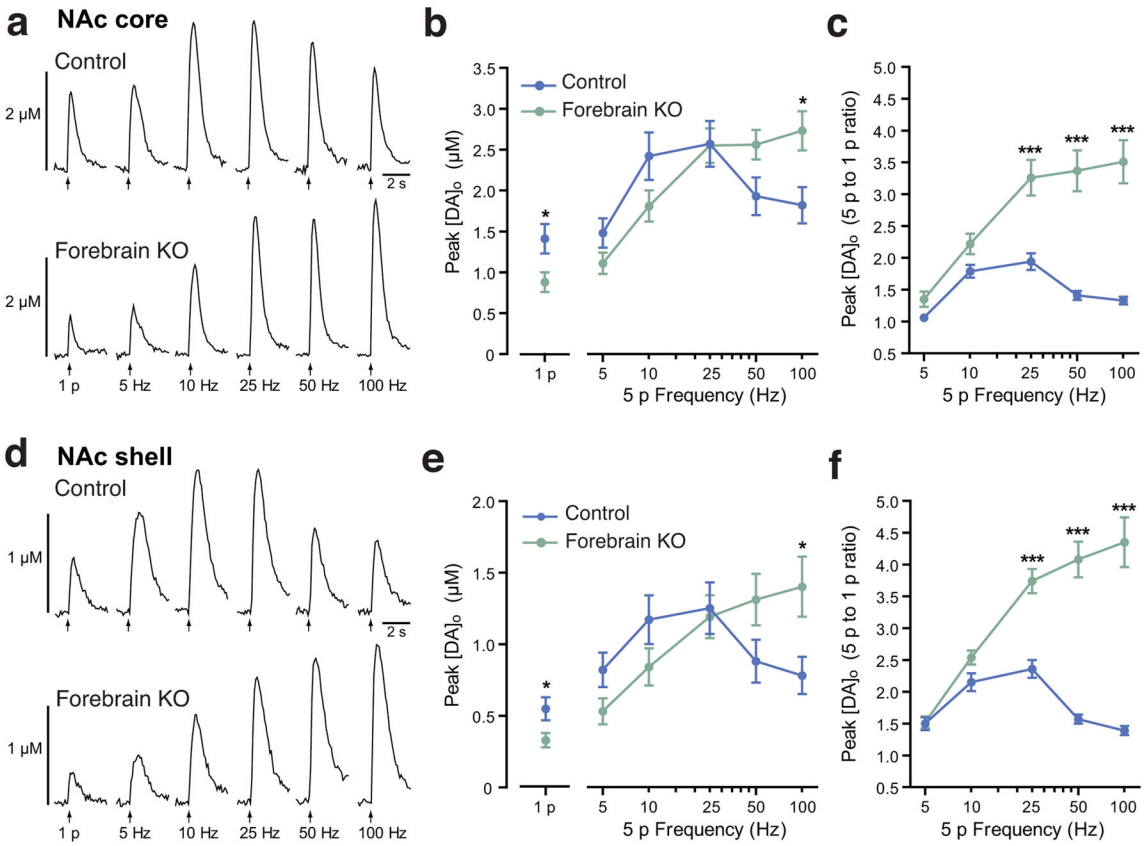


**Figure 3.**

Loss of forebrain ACh production results in enhanced phasic-to-tonic DA signaling within the ventral striatum. (**a–f**) Voltammetric monitoring of extracellular DA concentration ($[DA]_o$) in the nucleus accumbens (NAc) of striatal slices. (**a,d**) Representative single-pulse (1 p) and five-pulse (5 p) evoked $[DA]_o$ recorded in non-mutant control and forebrain KO mice in the NAc core (**a**) and NAc shell (**d**). (**b,e**) Mean peak $[DA]_o$ evoked by 1 p and 5 p stimulation in each group shows suppression of DA release up to 10 Hz (*p<0.05 *vs.* control for 1p; unpaired t-test or two-way ANOVA with Bonferroni correction for comparison of 5 p), maintenance of release levels at 25 Hz and, enhanced peak $[DA]_o$ at 50 Hz and 100 Hz (*p<0.05; *vs.* control for 100 Hz; two-way ANOVA with Bonferroni correction) in both the NAc core (**b**) and NAc shell (**e**). (**c,f**) Frequency dependence (5 p to 1 p ratio) of evoked $[DA]_o$ in control and forebrain KO mice under control conditions. The 1 p-to-5 p ratios in forebrain KO mice were enhanced at frequencies above 25 Hz (***p<0.001 for each frequency, two-way ANOVA with Bonferroni correction) in both the NAc core (**c**) and NAc shell (**f**) indicating enhanced phasic-to-tonic DA signaling throughout the ventral striatum with loss of ACh. Data for NAc core are from 3 control mice and 3 forebrain KOs with n=14 recording sites in each. Data for NAc shell are from 3 control mice with n=9 recording sites and 3 forebrain KOs with n=11 recording sites. All data are means ± SEM.

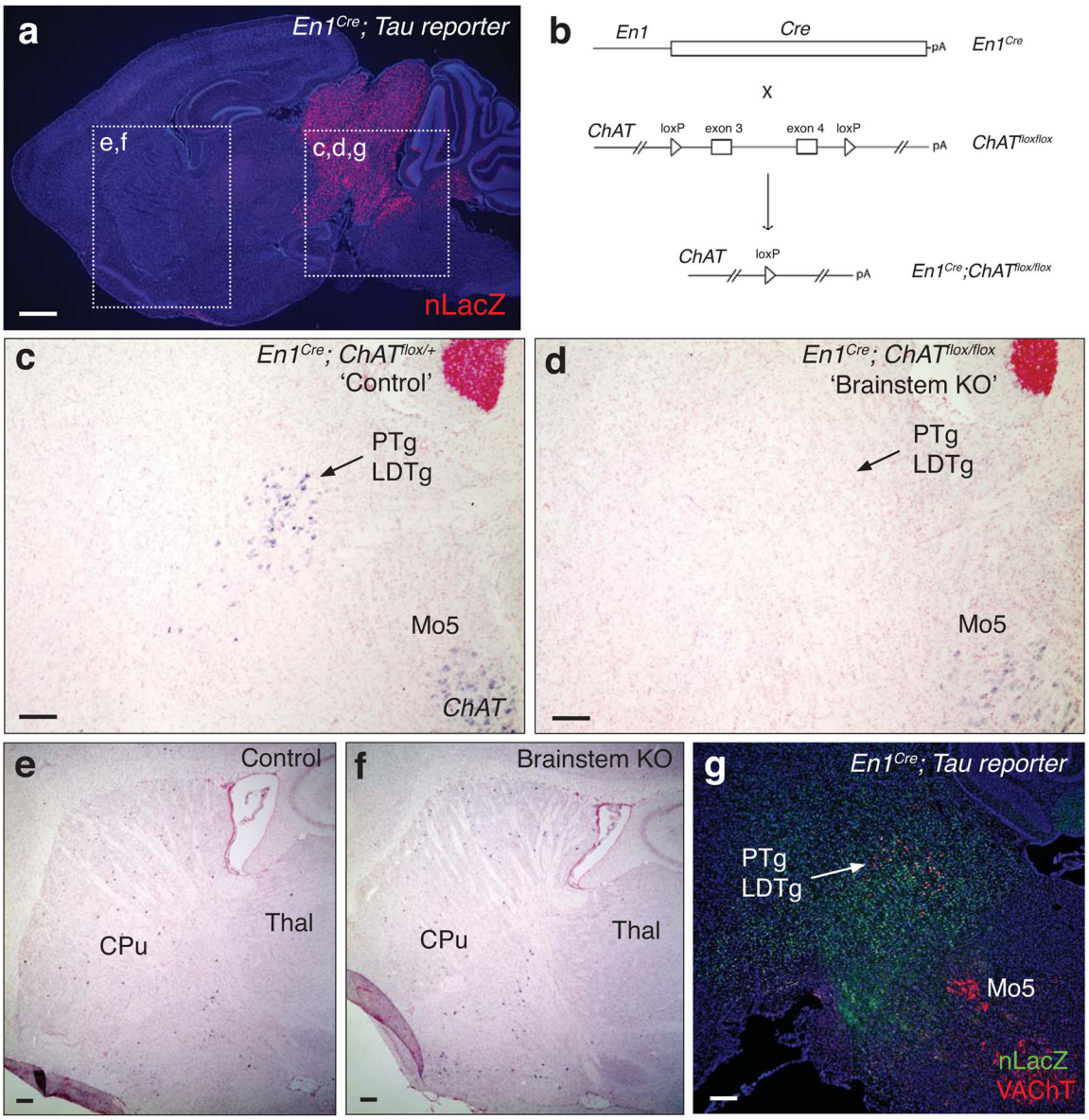


**Figure 4.**

Genetic strategies for targeted ablation of ACh production in the rostral brainstem (**a**) Sagittal field of a P21 *En1*$^{Cre}$*; Tau*$^{loxP\text{-}stop\text{-}loxP\text{-}mGFPiresNLSLacZ}$ (‘*Tau reporter*’) mouse brain illustrating the populations (nLacZ$^{+}$; red) that arise from *En1* expressing lineages. (**b**) Genetic strategy for selective elimination of ACh production within the rostral brainstem (*En1* lineages). (**c–d**) *In situ* hybridization for *ChAT* mRNA in sagittal brainstem cryosections from *En1*$^{Cre}$*; ChAT*$^{flox/+}$ non-mutant control (**c**) and *En1*$^{Cre}$*; ChAT*$^{flox/flox}$ brainstem KO (**d**) mice at P30 revealed a complete loss of *ChAT* expression in the PTg/LDTg of the brainstem KO, but normal *ChAT* expression in Mo5. (**e–f**) Sagittal fields of control (*En1*$^{Cre}$*; ChAT*$^{flox/+}$; **e**) and mutant (‘brainstem KO’; *En1*$^{Cre}$*; ChAT*$^{flox/flox}$; **f**) P30 forebrain sections stained by *in situ* hybridization for *ChAT* mRNA reveals normal *ChAT* expression in the forebrain of brainstem KO mice. (**g**) Sagittal field of a P21 *En1*$^{Cre}$*; Tau*

*reporter* brain section stained by immunohistochemistry for nuclear β-galactosidase (nLacZ; green) and vesicular acetylcholine transporter (VAChT; red) reveals complete labeling of the PTg/LDTg but no labeling within Mo5. PTg, pedunculopontine nucleus; LDTg, laterodorsal tegmental nucleus; Mo5, motor trigeminal nu; CPu, caudate putamen; Thal, thalamus. Scale bar in (**a**) represents 1 mM; scale bars in (**c–g**) represent 300 μM.

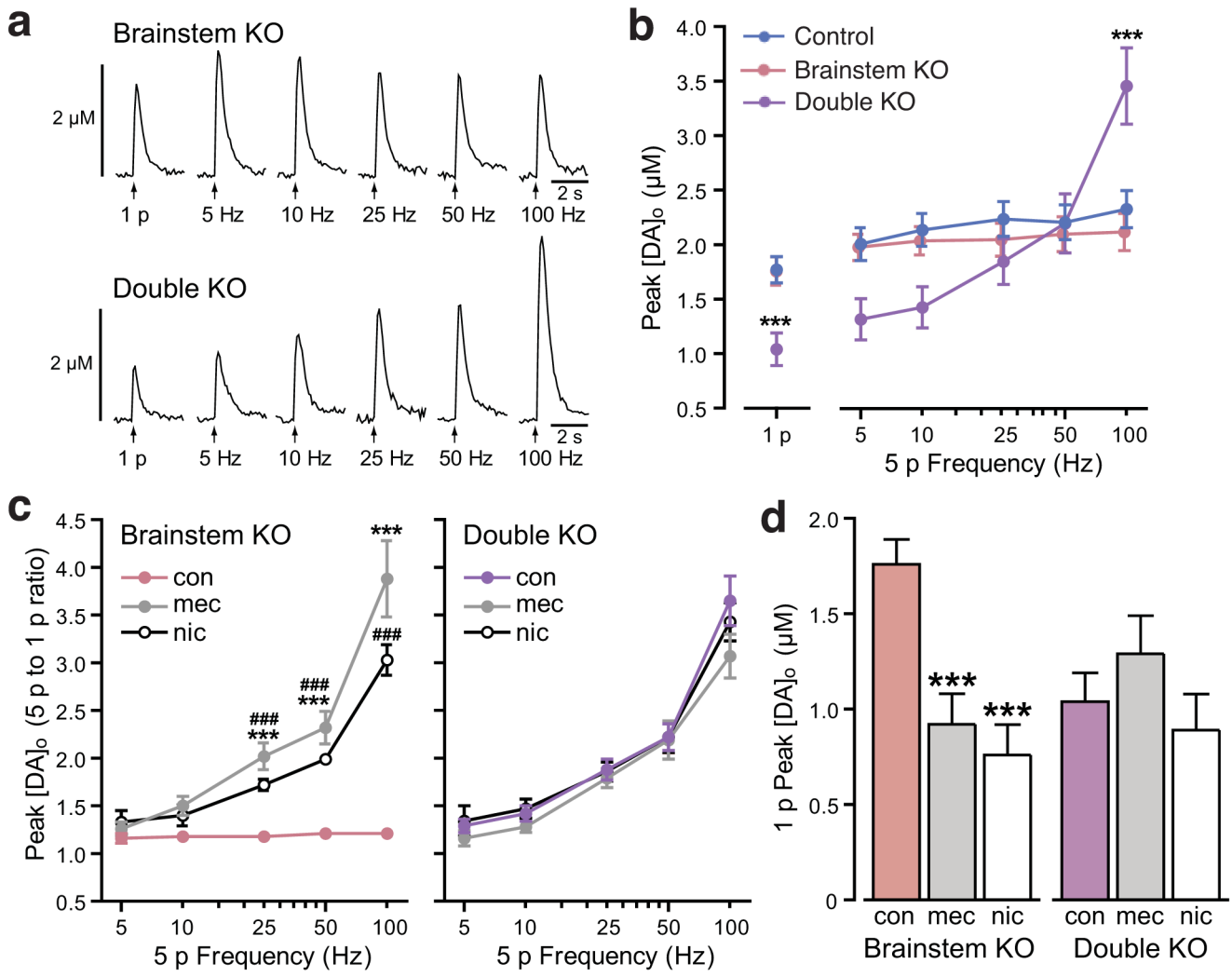


**Figure 5.**

Loss of brainstem derived ACh does not affect local regulation of striatal DA release. (**a–d**) Voltammetric measurements of extracellular DA concentration ($[DA]_o$) in the caudate putamen (CPu) of striatal slices. (**a**) Representative single-pulse (1 p) and five-pulse (5 p) evoked $[DA]_o$ recorded in brainstem KO and forebrain/brainstem double KO mice. (**b–c**) Mean peak $[DA]_o$ evoked by 1 p and 5 p stimulation shows that DA release is not significantly altered in brainstem KO *versus* control mice (**b**). In double KO mice, there is a general suppression of DA release up to 10 Hz, maintenance of release levels at 25 and 50 Hz, and enhanced peak $[DA]_o$ at 100 Hz (**b**) (***p<0.001 *vs* control; unpaired t-test for comparison of 1 p or two-way ANOVA with Bonferroni correction for comparison of 5 p). (**c**) Frequency dependence (5 p-to-1 p ratio) of evoked $[DA]_o$ in brainstem and double KO mice under control conditions (con) and in the presence of the nAChR antagonist mecamylamine (mec, 5 µM) or a desensitizing concentration of nicotine (nic, 500 nM) (***p<0.001 mec *vs.* con, ###p<0.001 nic *vs.* con, two-way ANOVA with Bonferroni correction). The 1 p to 5 p ratio in double KO mice under control conditions was indistinguishable from those seen in control mice in mec or nic (p>0.05 for each frequency

for either mec or nic, two-way ANOVA with Bonferroni correction). (**d**) 1 p evoked $[DA]_o$ in double KO mice was not suppressed by either mec or nic, in contrast to brainstem KO mice (***p<0.001 *vs*. con, one-way ANOVA with Dunnett's correction). Data for brainstem KOs are derived from 4 mice with n=16 recording sites in control conditions and n=8 sites in each drug. Data for double forebrain/brainstem KOs are derived from 4 mice with n=16 recording sites in control conditions, n=7 sites in mec and n=9 sites in nic. All data are means ± SEM.

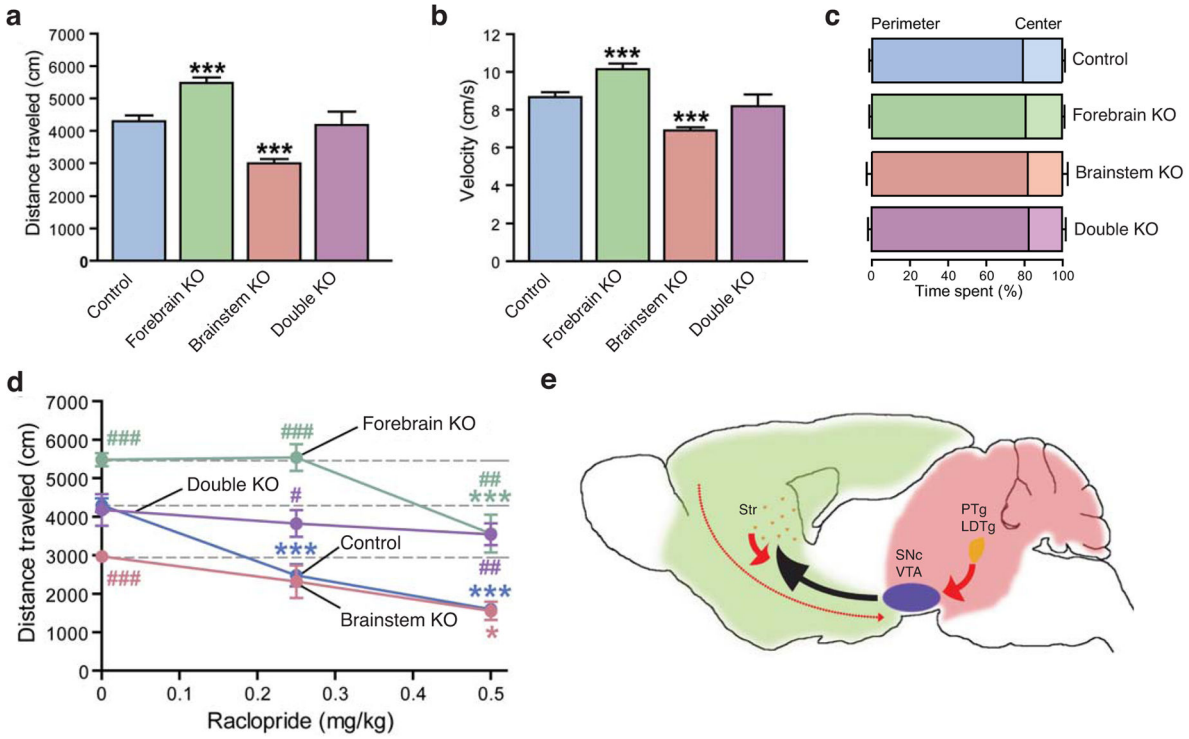


**Figure 6.**

Hyperactivity in forebrain ACh KO mice is normalized by D2R antagonism or by loss of brainstem ACh. (**a–b**) Summary of open field activity showing changes in total distance traveled/10 min assay (**a**) and velocity of movement in control (**b**) (n=26), forebrain KO (n=12), brainstem KO (n=14), and forebrain/brainstem double KO (n=8) mice, ***p<0.001 *vs.* control, one-way ANOVA with Dunnett's correction. (**c**) Loss of brain ACh does not alter anxiety-related behavior in the open field arena. There were no significant differences in the time spent in the center *versus* perimeter zones during the first 10 min in the arena between non-mutant control (n=26), forebrain KO (n=12), brainstem KO (n=14), and forebrain/brainstem double KO (n=8) mice, p>0.05 *vs.* control, one-way ANOVA with Dunnett's correction (**d**) Titration of raclopride dosage reveals the hyperdopaminergic phenotype of forebrain cholinergic mutants (n=4–12) *versus* control (n=5–26). Raclopride has little effect on locomotor activity when brainstem ACh is removed suggesting lower D2 receptor activation in hypoactive brainstem KO mice (n=4–14) than in control mice. Double KO mice exhibit a similar insensitivity to raclopride to that seen in brainstem KO mice (n=6–8). *p<0.05; ***p<0.001 *vs.* 0 mg/kg in each mouse group, one-way ANOVA with Bonferroni correction; $^{\#\#}$p<0.01;$^{\#\#\#}$p<0.001 *vs.* control mice, two-way ANOVA with Bonferroni correction. (**e**) Sagittal schematic depicting a model for coordinate regulation of DA release at the presynaptic level by striatal cholinergic interneurons (green territory) and at the soma by PTg/LDTg cholinergic projection neurons (red territory) as well as by descending forebrain projections from the prefrontal cortex, ventral pallidum, and hippocampus (green territory). All data are means ± SEM.